Cyclotron Resonance of the Two-Dimensional Electron Crystal

L. Wilen[a] and R. Giannetta
Department of Physics, Princeton University, Princeton, New Jersey 08543
(Received 10 September 1987)

Cyclotron-resonance measurements of surface-state electrons on liquid helium are reported. By independently controlling the electron density and electric field, we identify the contribution to the conductivity from many-electron effects. The linewidth increases with density, in conflict with existing theories. The onset of electron crystallization is not observed with cyclotron resonance.

PACS numbers: 71.45.Gm, 73.20.Dx, 73.25.+i, 76.40.+b

Coulomb forces can strongly influence the physics of two-dimensional (2D) electronic systems at low temperatures. For nondegenerate electrons on the liquid-helium surface, Wigner crystallization is a dramatic example.[1] One may ask how these many-body effects manifest themselves in various transport processes. We explore this question using cyclotron resonance as a probe of the electrical conductivity. Our experiment represents a significant extension of earlier work[2] in that (1) the electron density is controlled independently of other parameters, (2) Coulomb effects modify single-particle behavior at all densities studied, (3) temperature dependence of the cyclotron absorption is measured, and (4) we experimentally determine the role of crystallization.

At low temperatures ($T < 0.5$ K), electronic momentum loss occurs through interactions with the quantized vibrations of the helium surface, known as ripplons. This interaction takes the form of a deformation potential whose coupling constant, $V_{\mathbf{q}}$, is given by[3]

$$V_{\mathbf{q}} = (\hbar q/2\omega_q \rho)^{1/2}[eE_\perp + P(q)], \quad (1)$$

where ω_q is the ripplon frequency at wave vector $\mathbf{q}$ and ρ is the helium density. $E_\perp = (E^> + E^<)/2$ is the effective static electric field where $E^>$ and $E^<$ are fields immediately above and below the charge layer. $P(q)$, known as the polarization interaction, arises from the curvature of the liquid surface and is independent of applied fields. Expression (1) accurately accounts for many features of the electronic transport on the helium surface.[4] However, recent experiments have indicated that the total scattering rate increases with electron density, n_s.[5] Such many-body effects are identified by a dependence upon n_s over and above that trivially contained in $E_\perp$. In order to explore these effects systematically, it is necessary to depart from the saturation condition, $E_\perp = 2\pi n_s e$, employed in previous experiments. Using a capacitive technique described elsewhere, we control $E_\perp$ and n_s independently.[6] This procedure allows us to separate electron-ripplon from density-dependent interactions.

Our experimental cell is shown in Fig. 1. Charge is deposited onto the helium surface by the illumination of a Zn-coated sapphire photoemitter with uv light from a quartz optical fiber. Electrons are confined in a circular pool by the application of independent potentials to the top, side, and bottom walls. Both top and bottom plates are Corbino electrodes. The lower electrode's impedance is monitored with a capacitance bridge operating at 30 kHz in order to determine the electron density, the plasma frequency, and the magnetoresistance of the charge pool. The top electrode forms the capacitance element of a 2-GHz hybrid resonator operating in a transmission mode. The cavity measures the surface impedance at the cyclotron frequency. Microwave power to the cavity power is held below 10^{-13} W to avoid heating of the electrons. (Electron heating is first indicated by a change in the mass shift with input power.) The cell temperature is regulated with a carbon resistor, and calibrated against an *in situ* ^{3}He melting-curve thermometer.

Inserting a Lorentzian form for the surface conductivity near resonance into our expression for the cavity impedance,[7] we obtain an expression for the absorptive response of the resonator in the presence of surface-state electrons:

$$\Delta G = \Gamma[\Gamma^2 + (\omega - \omega_c - \delta\omega - \omega_p^2/2\omega_c)^2]^{-1}, \quad (2)$$

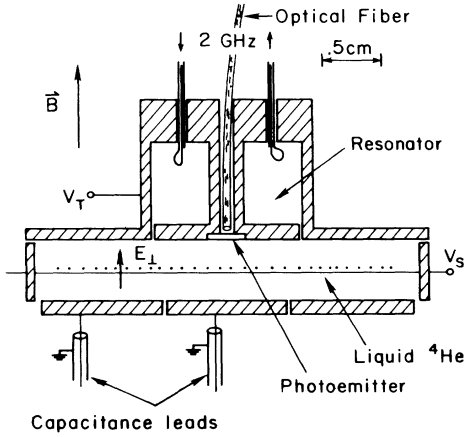

FIG. 1. Experimental cell.

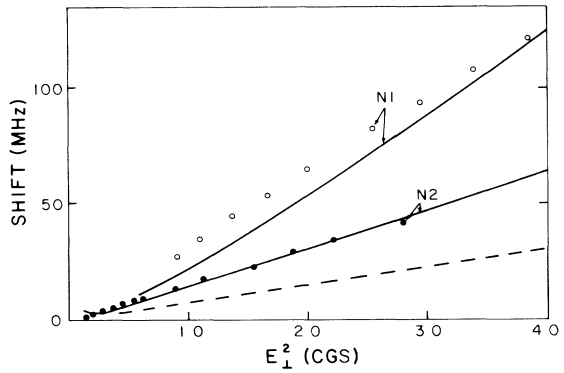

FIG. 2. Frequency shift vs $E_\perp^2$. $N1$ and $N2 = (3.7$ and $0.96) \times 10^8/\text{cm}^2$, respectively. Dashed line is the shift from Eq. (3). Solid curves represent theory from Ref. 9, corrected for polarization interaction, for $\mu = 1.6$. $T = 80$ mK.

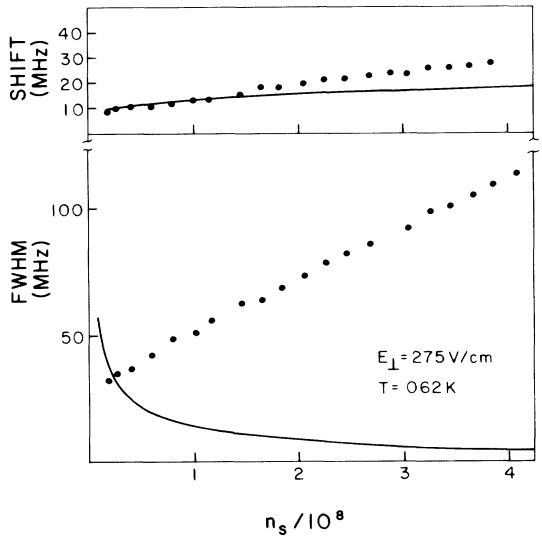

FIG. 3. Top: Frequency shift vs n_s. Bottom: Linewidth vs n_s. Solid curves represent theory from Ref. 9 for $\mu = 1.6$.

where $\delta\omega$ and Γ represent the frequency shift and linewidth of the cyclotron resonance due to the physical processes under investigation. ω_p is the plasma frequency ($\simeq 120$ MHz at $n_s = 10^8/\text{cm}^2$) and ω_c is the free-electron cyclotron frequency. Our experimental magnetic field sweeps are fitted by the form (2). For all results shown, the magnetoplasma shift, $\omega_p^2/2\omega_c$, has been subtracted from the raw data.

An isolated electron coupled to the surface through (1) will exhibit a shift away from the bare cyclotron frequency by approximately,

$$\hbar\delta\omega = \hbar(\omega - \omega_c) = (eE_\perp)^2/4\pi\sigma, \tag{3}$$

where σ is the helium surface tension. The shift arises from the deformation of the helium surface beneath each electron which forces different Landau levels to acquire slightly different values of $\langle z \rangle$, the mean vertical distance between the electron and the helium surface ($\simeq 75$ Å).[8] In the presence of a vertical electric field, $E_\perp$, the energy spacing of the lowest two Landau levels will then be given by $\hbar(\delta\omega + \omega_c)$. As the electron density is increased, the independent-particle picture becomes inadequate. We illustrate this point in Fig. 2. The shift is plotted versus $E_\perp^2$ for two different electron densities. Equation (3) is plotted as a dashed line for comparison. It is clear that the shift is a strong function of the electron density, irrespective of other parameters. We illustrate this point more clearly in Fig. 3 (top) where $E_\perp$ is held fixed but n_s is varied.

Shikin[10] has argued that Coulomb effects become important when the magnetic length, $l = (c\hbar/eB)^{1/2} \approx 1200$ Å, exceeds the amplitude of zero-point motion, $\langle u^2 \rangle^{1/2}$. An equivalent statement is that the zone-boundary plasma frequency, $\Omega_p = (2\pi e^2/m)^{1/2} n_s^{3/4}$, should exceed the cyclotron frequency, ω_c. For our data, $0.5 \lesssim \Omega_p/\omega_c \lesssim 9.2$. To date, the most complete theory of cyclotron resonance in a 2D electron crystal is due to Dykman.[9] In the limit $\Omega_p/\omega_c \gg 1$, this theory yields a Coulomb-enhanced frequency shift whose temperature-independent component is given by

$$\hbar\delta\omega = \frac{e^2}{4\pi\sigma}\frac{\Omega_p}{\mu\omega_c}(E_\perp^2 + E_\perp g_1 + g_2), \tag{4}$$

where $\mu \approx 1.6$ is a density-independent parameter proportional to the zero-point amplitude. g_1 and g_2 are corrections from the polarization field.[11] The full shift also contains a temperature-dependent component proportional to the linewidth. The full shift, including these corrections, is plotted as a solid line in Fig. 2, and in Fig. 3 (top). Despite some difference at higher densities, the data are in qualitative agreement with the theory.

Investigation of the linewidth reveals a serious discrepancy with theory. To order ω_c/Ω_p the width is given by

$$\pi W = \Gamma = \frac{e^2}{16\pi\sigma\mu^2}\frac{k_B T}{\hbar\omega_c}\frac{\Omega_p^2}{c_t^2 n_s}\left(E_\perp^2 + f_1 E_\perp + f_2 + \frac{\Omega_p^2\omega_c}{c_t^2 n_s 4\pi\mu\Omega_p}(E_\perp^2 + h_1 E_\perp + h_2)\right), \tag{5}$$

where W is the FWHM, c_t is the transverse sound velocity, and f_1, f_2, h_1, and h_2 are contributions from the polarization interaction.[11] This expression is plotted along with the data in the lower portion of Fig. 3. It is clear, however, that the experimental linewidth exhibits an unambiguous *increase* with electron density. This rather striking disparity is also evident if we plot the width versus $E_\perp$ for three different densities, as in Fig. 4. The solid lines are fits by the

form

$$\Gamma_{\text{expt}} = \frac{e^2}{16\pi\sigma\mu^2}\frac{k_B T}{\hbar\omega_c}\frac{\Omega_p^2}{c_t^2 n_s}(E_\perp^2 + 0.66E_\perp + 0.29) + \delta\Gamma(n_s, T), \quad (6)$$

where $\delta\Gamma$ depends upon n_s. Experimentally then, the density dependence appears as an additive offset $\delta\Gamma(n_s,T)$ which *increases* with n_s and is independent of $E_\perp$. (The fact that the data sets extend down to different electric fields reflects our inability to confine charge at arbitrary combinations of $E_\perp, n_s$.) We note that although Edel'man did not systematically explore the high-density regime, his linewidth data are consistent with our own.[2]

For a homogeneous system, electron-electron collisions cannot provide a contribution to the linewidth that is independent of processes which degrade the total electronic momentum.[12] The fact that (6) yields a respectable fit to the data suggests that an additional dissipative mechanism exists which depends upon a parameter other than $E_\perp$ over which we have no direct experimental control.

We have undertaken numerical simulations of the cavity impedance in order to check for possible inhomogeneous broadening from the edges of the charge pool. Our calculated resonance line shape exhibits no observable inhomogeneous broadening. We find no experimental evidence for an asymmetric line shape that would result from the reduced frequency shifts near the edges. (Note that all measurements are taken by our capacitively monitoring the charge pool diameter and then adjusting plate voltages to maintain constant diameter.) Furthermore, we find that the magnetoplasma shift is characteristic of a single wave vector ($k \approx 6$) regardless of the $(E_\perp, n_s)$ combination. This result rules out spurious broadening due to multiple plasma resonances. The spectrometer response is linear over more than four decades precluding nonlinearity as a source of broadening.

Finally, we illustrate in Fig. 5 the temperature dependence of the cyclotron absorption. Although the Wigner transition (marked by arrows) could be observed in the magnetoresistance, measured at 30 kHz, it was not apparent from the cyclotron resonance signal. The linewidth exhibits a clear change near $T = \hbar\omega_c/k_B$, below which it begins to vary linearly with temperature in agreement with (5). The dashed lines in Fig. 5 are simply linear extrapolations of the data to $T = 0$. It appears that the increase in linewidth with density is actually larger for $T > \hbar\omega_c/k_B$. Temperature dependence in the frequency shift is somewhat weaker than predicted, as shown by the solid line in Fig. 5 (top).

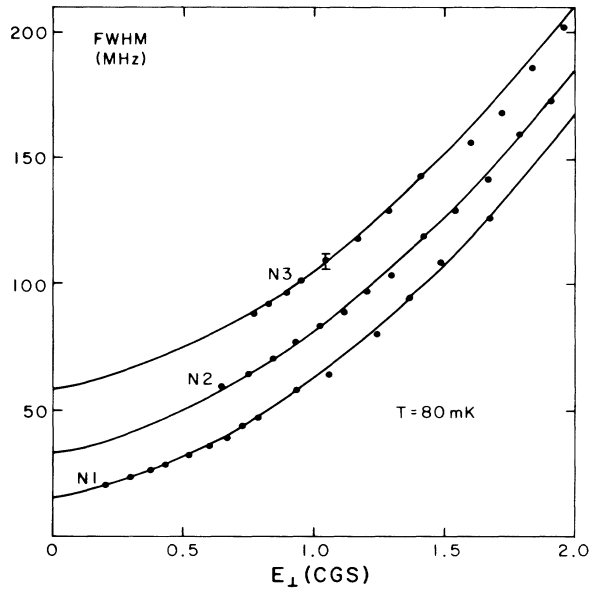

FIG. 4. Linewidth vs $E_\perp$ for densities $N1, N2, N3 = (0.96, 2.2, 3.6) \times 10^8/\text{cm}^2$. Solid curves are fits using Eq. (6). $T = 80$ mK.

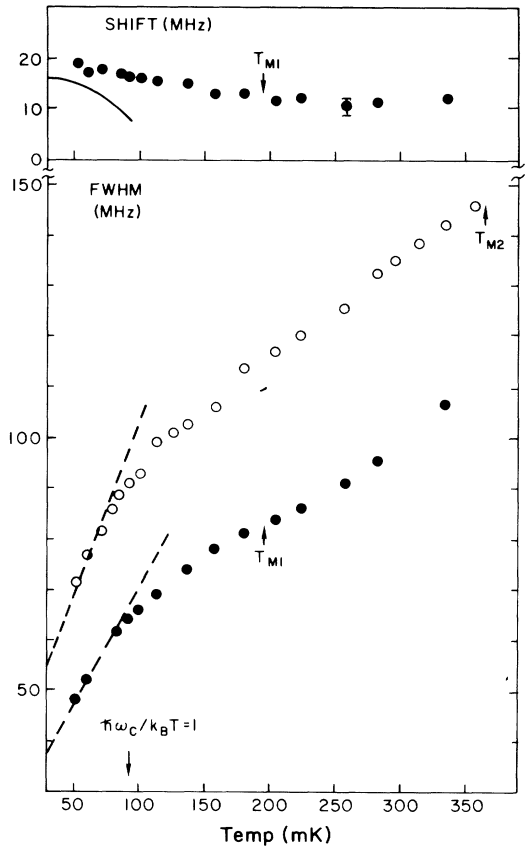

FIG. 5. Frequency shift and linewidth vs temperature. Melting transition occurs at T_M. Solid line is prediction from Ref. 9 for $\mu = 1.6$. Dashed lines are guides to the eye extrapolated to the origin. (Open circles, $n_s = 2.6 \times 10^8/\text{cm}^2$, $E = 1.05$ cgs; filled circles, $n_s = 0.75 \times 10^8/\text{cm}^2$, $E_\perp = 0.98$ cgs.)

In conclusion, we find that the cyclotron-resonance linewidth exhibits an unexplained increase with electron density. Calculations which utilize the conventional form of the electron-ripplon interaction are at odds with the observed behavior.[9,13] The behavior of the line shift is in reasonable agreement with theory. At our level of sensitivity, the onset of crystallization is not observable with cyclotron resonance.

We wish to thank J. Jensen, J. Sauls, D. Tsui, A. Dahm, F. I. B. Williams, S. Trugman, P. M. Platzman, B. Halperin, and M. Saitoh for useful discussions, E. Polturak for a careful reading of the manuscript, and T. R. Chien for assistance in the early stages of this experiment. This work was supported by the National Science Foundation under Contract No. DMR-8519339 and by the Research Corporation under Grant No. 9823. One of us (L.W.) acknowledges receipt of an IBM postdoctoral fellowship.

[a]Present address: Department of Physics, Technion–Israel Institute of Technology, 32000 Haifa, Israel.

[1]C. C. Grimes and G. Adams, Phys. Rev. Lett. **42**, 795 (1979).

[2]V. S. Edel'man, Zh. Eksp. Teor. Fiz. **77**, 673 (1979) [Sov. Phys. JETP **50**, 338 (1979)].

[3]V. B. Shikin and Yu. P. Monarka, J. Low Temp. Phys. **16**, 193 (1974).

[4]P. M. Platzman and G. Beni, Phys. Rev. Lett. **36**, 626 (1976).

[5]R. Mehrota, C. Guo, Y. Ruan, D. Mast, and A. Dahm, Phys. Rev. B **29**, 5239 (1984).

[6]L. Wilen and R. Giannetta, to be published.

[7]The absorptive response for our resonator is given by

$$\Delta G=\frac{(4\pi k/\omega)\mathrm{Re}\sigma_{xx}(k,\omega)}{[(4\pi k/\omega)\mathrm{Re}\sigma_{xx}(k,\omega)]^2+[f^{-1}(k)-(4\pi k/\omega)\mathrm{Im}\sigma_{xx}(k,\omega)]^2},$$

$$f(k)\equiv\coth kd+\coth kh,$$

where h and d are distances from the liquid surface to the top and bottom electrodes, respectively. σ_{xx} is the conductivity.

[8]A. Cheng and P. M. Platzman, Solid State Commun. **25**, 813 (1978).

[9]M. I. Dykman, J. Phys. C **15**, 7397 (1982).

[10]V. B. Shikin, Zh. Eksp. Teor. Fiz. **77**, 717 (1979) [Sov. Phys. JETP **50**, 361 (1978)].

[11]Using the notation of Ref. 9 we obtain

$$g_1=\frac{E_H l^2}{2n}(3+\gamma-2\ln 4\gamma_0 n^{1/2}),\quad g_2=\left(\frac{E_H l^2}{2n}\right)^2[7.354-(7+2\gamma)\ln 4\gamma_0 n^{1/2}+2(\ln 4\gamma_0 n^{1/2})^2],$$

$$f_1=\frac{E_H l^2}{2n}(7+2\gamma-4\ln 4\gamma_0 n^{1/2}),\quad f_2=\left(\frac{E_H l^2}{2n}\right)^2[42.47+17\gamma-(46+12\gamma)\ln 4\gamma_0 n^{1/2}+12(\ln 4\gamma_0 n^{1/2})^2],$$

$$h_1=\tfrac{3}{2}f_1+E_H l^2/2n^2,\quad h_2=2f_2-\tfrac{1}{4}(E_H l^2/2n)^2(12\ln 4\gamma_0 n^{1/2}-23-6\gamma).$$

The temperature correction to the shift is given by

$$\delta\omega(T)=2\Gamma_1\ln\left(\frac{\hbar\omega_c}{k_B T}\right),\quad \Gamma_1=\frac{e^2}{16\pi\sigma\mu^2}\frac{k_B T}{\hbar\omega_c}\frac{\Omega_p^2}{c_t^2 n_s}(E_\perp^2+f_1 E_\perp+f_2),$$

$$\gamma=0.577,\quad n=\mu\hbar/2m\Omega_p,\quad \gamma_0^{-1}=71\ \text{Å},\quad E_H=\gamma_0\hbar^2/me^2l^2,\quad \Omega_p^2/c_t^2 n_s=25.6.$$

[12]W. Kohn, Phys. Rev. **123**, 1242 (1961).

[13]V. V. Tatarskii, Fiz. Nizk. Temp. **11**, 451 (1985) [Sov. J. Low Temp. Phys. **11**, 245 (1985)].